VOL. 13, NO. 21, NOVEMBER 2018 ISSN 1819-6608
ARPN Journal of Engineering and Applied Sciences

www.arpnjournals.com

STUDY AND OPTIMIZATION OF A CAD/CFD MODEL FOR VALVELESS PULSEJETS

Luca Piancastelli[1], Stefano Cassani[2], Eugenio Pezzuti[3] and Luca Lipparini[1]
[1]Department of Industrial Engineering, Alma Mater Studiorum University of Bologna, Viale Risorgimento, Bologna (BO), Italy
[2]MultiProjecta, Via Casola Canina, Imola (BO), Italy
[3]Università di Roma "Tor Vergata", Dip. di Ingegneria dell'Impresa "Mario Lucertini", Via del Politecnico, Roma, Italy
E-Mail: luca.piancastelli@unibo.it

ABSTRACT

The method introduced in this paper aims to find a feasible method to evaluate the static thrust of a "valveless" pulsejet, starting from a CAD model. CFD (Computational Fluid Dynamic) simulation and golden section were used for this purpose. Even for new pulsejet designs, it is possible to evaluate the pulsating frequency from equations available in literature or with a mono-dimensional pressure wave model. Then the combustion energy should be introduced in the engine. In this CFD model, the heat flow due to the combustion is simulated through the application of a pulsating flow of hot gases through the walls of the combustion chamber. To minimize the error of this added flow, a stoichiometric combustion of pure oxygen is introduced. The temperature value of the hot gases was optimized with the Golden Section Method in order to obtain the same experimental results of the Department of Aerospace Engineering of California Polytechnic State University, San Luis Obispo [2]. In this way, it is possible to evaluate the performance of a new design of different geometry and size. In fact, a flow with the same temperature can be introduced through the wall of the combustion chamber. The mass flow rate can be trimmed to obtain a mass balance between the incoming and the outgoing gases. In this way, the thrust can be calculated. The fuel type is not very influent for pulsejet performance.

Keywords: pulsejet, static thrust, simulation, golden section, CFD.

PULSEJET

The Lockwood type pulsejet is an extremely simple design of a valveless jet engine in which combustion occurs intermittently providing a propulsion pulse. Unlike the ramjet/scramjet, the pulsejet is able to provide a boost at fixed point (TAS=0, True Air Speed).The pulsejet is an internal combustion engine, in which the intake air compression takes place dynamically, without the need of a compressor or of dynamic pressure. Unlike other jet engines, the combustion does not occur according to a continuous process, but to a pulse corresponding to each of the fuel injections in the system. Due the extensive work during and after WWII, a classical "low frequency" pulsejet is extremely easy to design starting from very few equations.

There are two basic categories of a pulsejet engine: the first category includes all those pulsejets in which the flow of gases is controlled by valves. As these valves allow the intake of fresh air into the combustion chamber, the pressure rise due to combustion leads to the closing of these valves constraining the exhaust gases to flow through a single discharge nozzle. Unfortunately, this type of pulsejet requires many more components than the valveless version, which result in a lower reliability, a higher cost of production and, in many cases, an extremely low TBO. The valve design is most critical. The second pulsejet category is the valveless pulsejet in which the gas flow is controlled exclusively by the fluid-dynamic principles of resonant flow. These types of pulsejet are commonly addressed as Lockwood type, due to the extensive work of this engineer from NACA. The pulsejet concept started in 1906 from the patent of the French (Russian born) engineer Victor Von Karavodin (also known as Victor De Karavodine). Georges Marconnet patented the valveless type in 1910.

The first significant pulsejet engine was the Argus AS 109-014 developed by Paul Schmidt for the V1 (buzz bomb). At the end of IIWW this engine was able to fly for less than half an hour with 640 lt of fuel and a maximum thrust of 2.7 kN [1-3].

The simplicity, low cost and effectiveness of the design impressed the Allies so much, so that they began to develop their own "low frequency" pulsejets. This research activity ended in the sixties due to lack of efficiency and limitations in thrust.

In 2006 the Russian company ENICS used a pulsejet engine in UAV applications. In particular, the pulsejet is used to equip a UAV drone, called E-95. The E-95 has the aim of simulating cruise missiles, bombs gliding, helicopters and attack aircraft. This application marks the first military use of a motor pulsejet since World War II.

In 1950 the FWE valveless VIII Twin Stacks was developed. It was based on the Chinese motor design CS. In the latter, the suction duct is directly connected to the combustion chamber with a 45° inclined section relative to the jet main axis. In the FWE VIII Twin Stack, evolution of the CS, a second symmetrical duct was added for additional suction capacity on the opposite side, obtaining a dual intake configuration. As a further improvement was the additional alternate converging to diverging sections along the longitudinal axis, to increase the efficiency (Figure-1). The aim of this paper is to model the version of the Chinese pulsejet FWE VIII Twin Stack to obtain the experimental results reported in [1-3] with Solid Works Flow Simulation and the Golden Section Method (Figure-2).

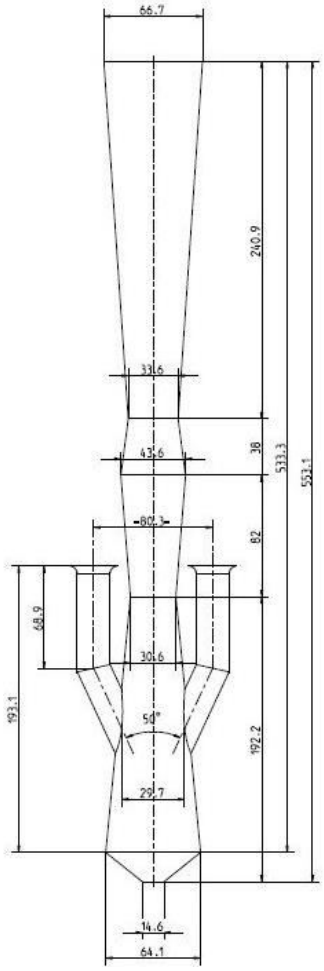

Figure-1. Drawing of the FWEVIII used for the CFD simulation.

Figure-2. Solid works CAD model.

The 3D CAD model of the FWE VIII Twin Stackis an assembly composed of five main parts: a central body, two side ducts and a connecting pipe inclined of 25 ° between the central body and the lateral ducts. The thickness of the sheet is 1mm (Figure-3).

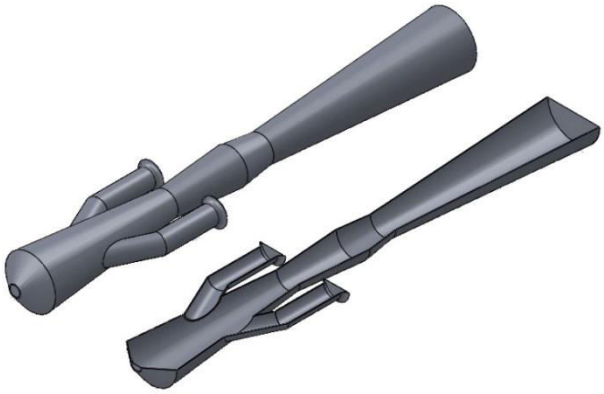

Figure-3. CAD model assembled.

In the central body an alternate divergent convergent sections pattern is adopted. This configuration allows optimum performance. This pulsejet is designed to maximize efficiency at (internal) supersonic speed. The pulsating pressure wave reverses the direction of a part of the hot gases causing them coming back into the combustion chamber. In this way, thanks to exhaust temperature, a priming of the propane-air mixture already sucked in the combustion chamber takes place. In a stationary duct, with constant mass flow rate of the incoming fluid, the following "Hugoniot" equations apply (1).

$$\frac{dA}{A} = \frac{dp}{\rho \cdot c^2}(1 - Ma^2)\frac{dA}{A} = \frac{dp}{\rho}\left(\frac{1-Ma^2}{Ma^2}\right) \quad (1)$$
$$\frac{dA}{A} = \frac{dp}{c}(Ma^2 - 1)$$

Where equation (2) holds.

$$Ma = \frac{c}{c_s} = \frac{c}{\sqrt{\gamma \cdot R \cdot T}} \quad (2)$$

CFD environmental and general assumptions

From the experimental conditions of report [2], the CFD simulations with the pulsejet are at ground level, TAS=0 (True Air Speed), ISA+0 (International Standard Atmosphere).The values of the environmental parameters are summarized in Table-1.

Table-1. Environmental.

Temperature	$T = 273{,}15\ °K$
Pressure	$p = 101325\ Pa$
Air Density	$\rho = 1{,}225\ kg/m^3$
TAS	$v = 0\ {}^{m}/_{s}$

CFD simulation

It was assumed to apply a pulsating heat flux on the combustion chamber external walls. This power application simulates the combustion process. The heat flow is easily inputted in the CFD by a hot mass flow through the combustion walls. The searched result is the

trust vs. time obtained by experiment [1-3]. A mass flow rate of combustion gases is therefore applied through the combustion chamber walls as in Figure-4.

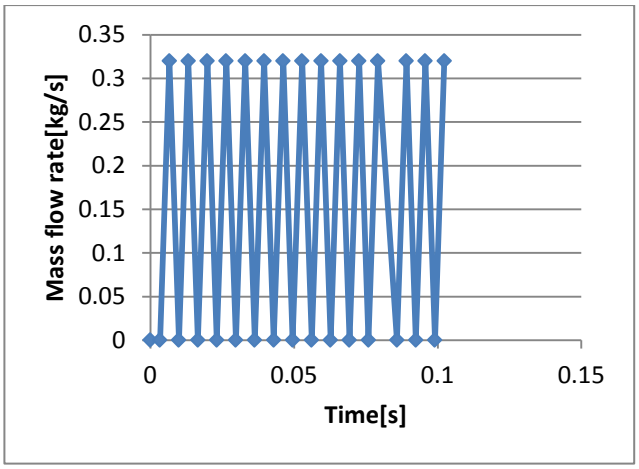

Figure-4. Mass flow rate of combustion gases on the combustion chamber walls.

To minimize the influence of this additional mass flow that is "unphysical", it was assumed to have a pure stoichiometric oxygen combustion. As regards to the internal flows resulting from the combustion process, it was assumed that the results (exhaust gas) of the chemical reaction between oxygen and propane gas are the production of CO_2 e H_20 in gaseous form.

The use of a complete combustion of propane gas gives equation (3).

$$C_3H_8 + 5O_2 \rightarrow 3CO_2 + 4H_20 \quad (3)$$

In terms of mass, equation (3) can be rewritten in equations (4).

$$m_{propane} + m_{o_2} = m_{CO_2} + m_{water} \Rightarrow \\ 44g + 160g = 132g + 72g \quad (4)$$

The starting information is the peak fuel flow (Fuel=0.069 kg/s) and the pulsating frequency (Freq=150 Hz). Therefore, if the combustion is purely stoichiometric the peak mass flow rate is given by equation (5).

$$Exhaust = Fuel + \frac{m_{o_2}}{m_{propane}} Fuel = 0.31[kg/s] \quad (5)$$

Then, it is possible to optimize the temperature by the golden section method. The target is to obtain the correct measured thrust. The pressure will come as a result of the CFD simulation. For the Golden Section Method, it is necessary to find maximum and minimum (feasible) temperatures. It is possible to evaluate a maximum possible temperature from the stoichiometric combustion of propane with air. The theoretical air a_t necessary for the combustion is given by the equations (6) (7) and (8):

$$x_c = \frac{C_3 m_{mC}}{C_3 m_{mC} + H_8 m_{mH}} = \frac{12.01 \times 3}{12.01 \times 3 + 1.008 \times 38} = 0.82 \quad (6)$$

$$x_H = \frac{H_2 m_{mC}}{C_3 m_{mC} + H_8 m_{mH}} = 0.18 \quad (7)$$

$$a_t = a_c x_c + a_H x_H = 11.5 x_c + 34.5 x_H = 15.7 \quad (8)$$

It is then possible to calculate the higher heating value of the propane (9).

$$HHV = 34.3 x_c + 144.42 x_H = 54.27[MJ/kg] \quad (9)$$

The LHV (lower heating value) is easily calculated from the mass fraction of H20 in exhaust per fuel mass (10).

$$LHV = HHV - 2.5 \frac{m_{water}}{m_{propane}} = 50.12[MJ/kg] \quad (10)$$

Therefore, the maximum temperature achievable from the combustion of propane and air is T_f=3,189 K (11).

$$T_f = T_a - \frac{LHV}{C_{pf} a_t} = 3189[K] \quad (11)$$

This is the upper limit of our simulation. The lower limit is the ambient temperature T_a=288.15 (ISA+0 s.l.). Due to this pulsating hot mass flow, the CFD calculates the temperature and pressure fields developed in the pulsejet. The wave pulse process is then simulated. In fact, the pulse (combustion) begins with the ignition of the air-fuel mixture in the combustion chamber. This chemical process causes a pressure and temperature increase in the combustion chamber, which gives life to a compression wave. This wave travels along both the suction port and discharge duct up to the speed of sound at the nozzle throat causing the expulsion of the burnt gas from the nozzle, thus providing the thrust. The wave of negative pressure in the intake ducts and the inertia of the exhaust gas in the main duct causes a pressure drop also in the combustion chamber thus triggering a new phase of fresh air intake.

When the compression wave reaches the reflecting part of each duct, it is reflected in the opposite direction as a low pressure wave. This happens first in the closest suction ports and then in the more distant discharge nozzle.

At the same instant, the output of the exhaust gas from the main duct causes a direct wave of depression towards the combustion chamber.

The rarefaction wave coming from the nozzle exhaust is transformed in a weak compression wave which transports the hot gas residues in again into the combustion chamber (backfire), thus triggering a new cycle, it is repeated typically between 40 and 250 times

per second (depending on the type and size of the engine). The ignition of the mixture can be controlled by a glow plug (typically on starting) or caused by backfire as just described.

Iterating the simulations, a convergence was reached with the following values around the values summarized in Table-2 (for the chemical reaction-air propane (3)). With the temperature of 973 K the thrust is the one find by reference [2]

Table-2. Data derived from experiments [2] and equation (3).

Average Exhaust Mass flow rate	0 .18 kg⁄s
Resonance frequency	150 Hz
Temperature in Combustion chamber TCFD	973 K
Max Pressure	1 .38 bar .

It is then possible to evaluate the true value of air to fuel ratio. A combustion efficiency η_c=0.95 is reasonable for propane combustion. An air excess *n* can be also added in equation (11). Therefore, equation (11) can be rewritten into equation (12).

$$T_{CFD} = T_a - \frac{\eta_c LHV}{C_{pf} a_t n} \quad (12)$$

It is then possible to evaluate the "true" air excess *n* (13)

$$n = \frac{\eta_c LHV}{C_{pf} a_t (T_{CFD} - T_a)} = 4 \quad (13)$$

This value of n is very high even for pulsating combustion. Therefore, it is possible that the fuel flow is limited by the maximum continuous temperature allowed for the materials than by the true thermodynamic limit of the pulsejet.

CFD results: velocity

Simulated velocity values (module) for the final section of the ducts are shown in Figure-5. In red for the main nozzle final section and in green the secondary, lateral nozzles. The initial transient is clearly visible in Figure-6. The two lateral duct contributes also to the total value of thrust. These ducts, being shorter than the main one, begin to suck air before the main duct.

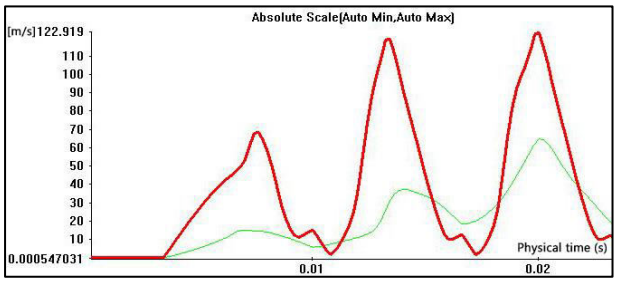

Figure-5. Velocity transient.

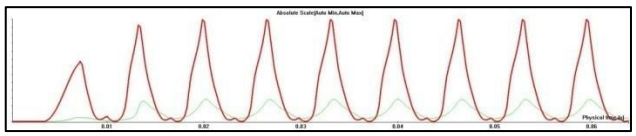

Figure-6. Velocity values becomes table.

Flow rate analysis

The main feature of this type of pulsejets is the capability to alternate the exhaust and the suction flows by using the resonating wave pressures, therefore avoiding any mechanical moving part (valveless). The alternation of the direction of the flows inside the side ducts is easily appreciated by observing Figure-7, where, the red line represents the mass flow in the side ducts. It was taken as a positive the incoming flow, (i.e. the flow of air necessary for combustion). The negative sign is the outgoing flow of combustion gases. In the green of the gas flow in the main duct [4-19].

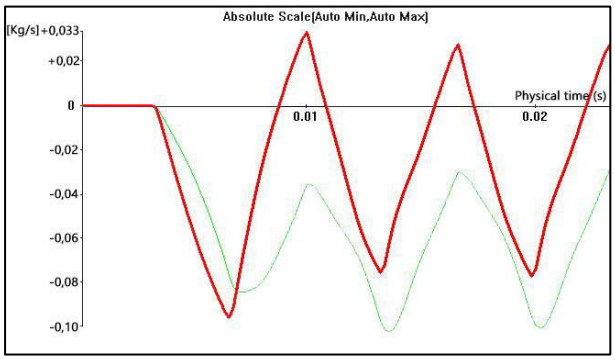

Figure-7. Mass flow in lateral ducts (red) and in central nozzle (green).

Pressure analysis

Figure-8 shows the pressure at lateral ducts (green) and at the main nozzle. (red). Pressure never goes under the atmosphere values due to ambient pressure constraint.

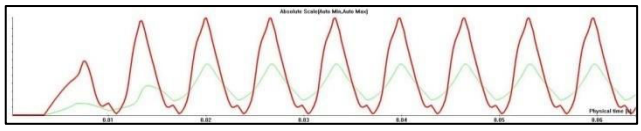

Figure-8. Dynamic pressures in the pulsejet (red-main duct, green-secondary ducts).

Dynamic pressures in the different phases of the cycle are shown in Figure-9.

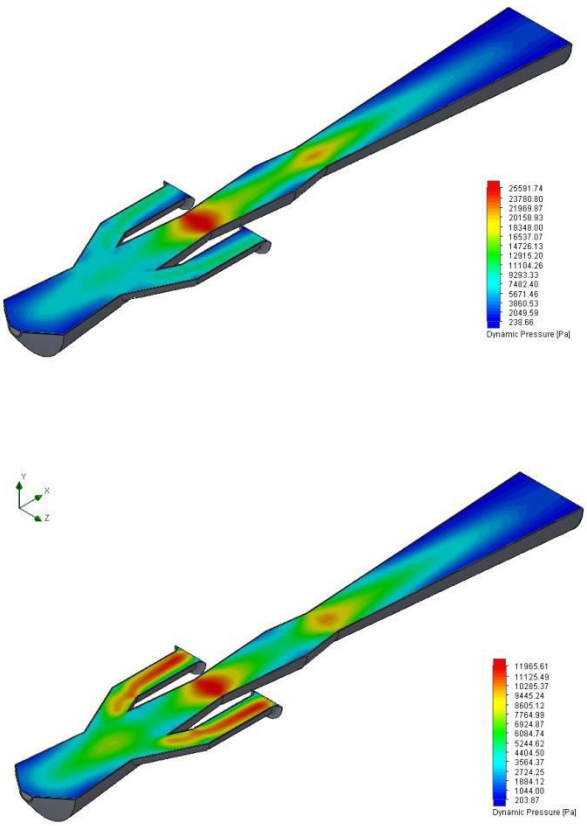

Figure-9. Pressure fields inside the pulsejet.

The pressure fields inside the pulsejet depend on the cycle phases that are different for the main duct and the secondary duct. In Figure-9 it is possible to see that the secondary duct nozzles are at peak pressure, while the primary duct nozzle is still at low pressure. Then the secondary nozzle pressure will drop, and the fresh air will enter inside the pulsejet. This intake air is dragged inside the computer by the fact that the main duct is still building pressure and the nozzle. This pressure build-up is done at the expense of a depression (negative pressure) inside the combustion chamber. Therefore, the different pressure-time scheduling makes it possible to suck air inside the combustion chamber through the secondary ducts. Then the back pressure from the main duct ignites the combustion and builds up the peak pressure in the combustion chamber.

Propulsion analysis

Finally, Figure-10 shows the results of the propulsive thrust obtained from equation (14).

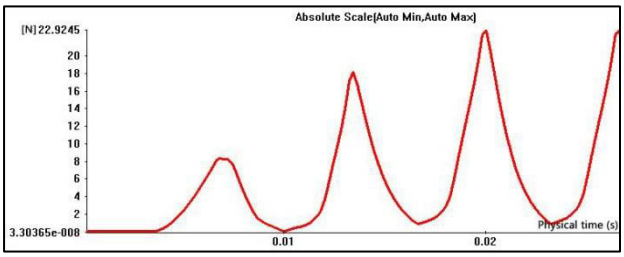

Figure-10. Thrust [N]vs time [s].

$$S = \sum_{i=1}^{3} \left(m_{pi} u_i + (p_{ei} - p_a) A_{ei} \right) \quad (14)$$

The thrust that was optimized through the Golden Section Method is the one experimentally by tests of the Department of Aerospace Engineering of California Polytechnic State University, San Luis Obispo [20-26]. They obtained a pulsating thrust with a maximum of 22.24 N. After the optimization; we obtained a maximum thrust of 22.92 N with the pulsating heat flux of Figure-4 with the parameters of Table-2. This result is considered acceptable by the authors.

CONCLUSIONS

The optimization method introduced in this paper aims to find a feasible model to calculate the static thrust of a "valveless" pulsejet, starting from a CAD model. For this purpose, CFD simulation is necessary. Even for new designs, it is possible to evaluate the pulsating frequency from equations available in literature or with a monodimensional pressure wave model. This paper starts from the experimental results of reference [2]. In this CFD model, the heat flow due to the combustion is simulated through the application of a pulsating flow of hot gases through the walls of the combustion chamber. To minimize the error of this added flow a stoichiometric combustion of pure oxygen was introduced. The temperature value of the hot gases was optimized in order to obtain the same experimental results of reference [2]. In this way it is possible to evaluate the performance of new design of different geometry and size. In fact, a flow with the same temperature can be introduced through the wall of the combustion chamber. The mass flow rate can be trimmed to obtain a mass balance between the incoming and the outgoing gases. In this way the thrust can be calculated. The fuel type is not very influent for pulsejet performance.

Symbols

Symbol	Description	Unit
A	Area of duct	m^2
ρ	Density	kg/ m^3
c	Speed	m/s
Ma	Speed of sound	m/s
R	Individual gas constant	J $kg^{-1}K^{-1}$
T	Temperature	K
$m_{propane}$	Molar mass propane	kg/mol
m_{O2}	Molar mass oxygen	kg/mol
m_{CO2}	Molar mass carbon dioxide	kg/mol
m_{water}	Molar mass carbon water	kg/mol
Exhaust	Mass flow into combustion chamber	kg/s
Fuel	Mass flow fuel (propane)	kg/s
a_t	Stoichiometric Air to fuel ratio in mass	-
T_f	Stoichiometric exaust temperature	K
C_{pf}	Specific heat capacity at constant pressure	$JK^{-1}kg^{-1}$
T_{CFD}	Temperature of hot gas flow from CFD and Golden Section	K
η_c	Combustion efficiency	-
p_{ei}	Exhaust pressure nozzle i	Pa
A_{ei}	Area nozzle i	m^2
u_i	Nozzle i speed	m/s
m_{pi}	Nozzle i mass flow rate	kg/s

REFERENCES

[1] L. Piancastelli, L. Frizziero, S. Marcoppido, E. Pezzuti. 2012. Methodology to evaluate aircraft piston engine durability edizioni ETS. International Journal of Heat & Technology ISSN 0392-8764, 30(1): 89-92, Bologna.

[2] L. Piancastelli, L. Frizziero, G. Donnici. 2015. The Meredith ramjet: An efficient way to recover the heat wasted in piston engine cooling. Asian Research Publishing Network (ARPN). Journal of Engineering and Applied Sciences. ISSN 1819-6608, 10(12): 5327-5333, EBSCO Publishing, 10 Estes Street, P.O. Box 682, Ipswich, MA 01938, USA.

[3] L. Piancastelli, A. Gatti, L. Frizziero, L. Ragazzi, M. Cremonini. 2015. CFD analysis of the Zimmerman's V173 stol aircraft. Asian Research Publishing Network (ARPN). Journal of Engineering and Applied Sciences. ISSN 1819-6608, 10(18): 8063-8070, EBSCO Publishing, 10 Estes Street, P.O. Box 682, Ipswich, MA 01938, USA.

[4] L. Piancastelli, L. Frizziero. 2014. Turbocharging and turbocompounding optimization in automotive racing. Asian Research Publishing Network (ARPN). Journal of Engineering and Applied Sciences. ISSN 1819-6608, 9(11): 2192-2199, EBSCO Publishing, 10 Estes Street, P.O. Box 682, Ipswich, MA 01938, USA

[5] L. Piancastelli, L. Frizziero, G. Donnici. 2014. The common-rail fuel injection technique in turbocharged di-diesel-engines for aircraft applications. Asian Research Publishing Network (ARPN). Journal of Engineering and Applied Sciences. ISSN 1819-6608, 9(12): 2493-2499, EBSCO Publishing, 10 Estes Street, P.O. Box 682, Ipswich, MA 01938, USA

[6] L. Piancastelli, L. Frizziero, G. Donnici, "Turbomatching of small aircraft diesel common rail engines derived from the automotive field", Asian Research Publishing Network (ARPN), "Journal of Engineering and Applied Sciences", ISSN 1819-6608, Volume 10, Issue 1, pp. 172-178, 2015, EBSCO Publishing, 10 Estes Street, P.O. Box 682, Ipswich, MA 01938, USA

[7] L. Piancastelli, L. Frizziero. 2015. Supercharging systems in small aircraft diesel common rail engines derived from the automotive field. Asian Research Publishing Network (ARPN). Journal of Engineering and Applied Sciences. ISSN 1819-6608, 10(1): 20-26, 2015, EBSCO Publishing, 10 Estes Street, P.O. Box 682, Ipswich, MA 01938, USA

[8] P.P.Valentini, E. Pezzuti E. Computer-aided tolerance allocation of compliant ortho-planar spring mechanism Int. Jou. Of Computer Applications In Technology, 53: 369-374, ISSN: 0952-8091, doi: 10.1504/IJCAT.2016.076801

[9] E. Pezzuti, PP. Valentini PP. Accuracy in fingertip tracking using Leap Motion Controller for interactive virtual applications Int. Jour. On Interactive Design And Manufacturing, pp. 1-10, ISSN: 1955-2513, doi: 10.1007/s12008-016-0339-y

[10] E.Pezzuti E, PP. Valentini P. Design and interactive simulation of cross-axis compliant pivot using dynamic spline. Int. Jour. On Interactive Design And Manufacturing. 7: 261-269, ISSN: 1955-2513, doi: 10.1007/s12008-012-0180-x

[11] L. Piancastelli, S. Cassani. 2017. Maximum peak pressure evaluation of an automotive common rail diesel piston engine head. Asian Research Publishing Network (ARPN). Journal of Engineering and Applied Sciences. ISSN 1819-6608, 12(1): 212-218, EBSCO Publishing, 10 Estes Street, P.O. Box 682, Ipswich, MA 01938, USA.

[12] S. Cassani. 2017. Airplane Design: The Superiority Of FSW Aluminum-Alloy Pure Monocoque Over CFRP "BLACK" CONSTRUCTIONS. Asian Research Publishing Network (ARPN). Journal of Engineering and Applied Sciences. ISSN 1819-6608, 12(2): 377-361, EBSCO Publishing, 10 Estes Street, P.O. Box 682, Ipswich, MA 01938, USA.

[13] L. Piancastelli, S. Cassani. 2017. Power Speed Reduction Units For General Aviation Part 2: General Design, Optimum Bearing Selection For Propeller Driven Aircrafts With Piston Engines. Asian Research Publishing Network (ARPN). Journal of Engineering and Applied Sciences. ISSN 1819-6608, 12(2): 544-550, EBSCO Publishing, 10 Estes Street, P.O. Box 682, Ipswich, MA 01938, USA.

[14] L. Piancastelli, S. Cassani. 2017. Power Speed Reduction Units For General Aviation Part 5: Housing/Casing Optimized Design For Propeller-Driven Aircrafts And Helicopters. Asian Research Publishing Network (ARPN). Journal of Engineering and Applied Sciences. ISSN 1819-6608, 12(2): 602-608, EBSCO Publishing, 10 Estes Street, P.O. Box 682, Ipswich, MA 01938, USA.

[15] L. Piancastelli, S. Cassani. 2017. Power Speed Reduction Units For General Aviation Part 3: Simplified Gear Design Piston-Powered, Propeller-Driven General AVIATION AIRCRAFTS. Asian Research Publishing Network (ARPN). Journal of Engineering and Applied Sciences. ISSN 1819-6608, 12(3): 870-874, EBSCO Publishing, 10 Estes Street, P.O. Box 682, Ipswich, MA 01938, USA.

[16] L. Piancastelli, S. Cassani. 2017. Power Speed Reduction Units For General Aviationpart 4: Simplified Gear Design For Piston-Powered, Propeller-Driven "Heavy Duty" Aircrafts And Helicopters. Journal of Engineering and Applied Sciences. ISSN 1819-6608, 12(5): 1533-1539, EBSCO Publishing, 10 Estes Street, P.O. Box 682, Ipswich, MA 01938, USA.

[17] L. Piancastelli, S. Migliano, S. Cassani. 2017. An Extremely Compact, High Torque Continuously Variable Power Transmission For Large Hybrid Terrain Vehicles. Journal of Engineering and Applied Sciences. ISSN 1819-6608, 12(6): 1796-1800, EBSCO Publishing, 10 Estes Street, P.O. Box 682, Ipswich, MA 01938, USA.

[18] L. Piancastelli, S. Cassani. 2017. Mapping Optimization For Partial Loads Of Common Rail Diesel Piston Engines. Journal of Engineering and Applied Sciences. ISSN 1819-6608, 12(7): 2223-2229, EBSCO Publishing, 10 Estes Street, P.O. Box 682, Ipswich, MA 01938, USA.

[19] L. Piancastelli, S. Cassani. 2017. High Altitude Operations With Piston Engines Power Plant Design Optimization Part V: Nozzle Design And Ramjet General Considerations. Journal of Engineering and Applied Sciences. ISSN 1819-6608, 12(7): 2242-2247, EBSCO Publishing, 10 Estes Street, P.O. Box 682, Ipswich, MA 01938, USA.

[20] L. Piancastelli, R. V. Clarke, S. Cassani. 2017. Diffuser Augmentedrun The River And Tidal Picohydropower Generation System. Journal of Engineering and Applied Sciences. ISSN 1819-6608, 12(8): 2678-2688, EBSCO Publishing, 10 Estes Street, P.O. Box 682, Ipswich, MA 01938, USA.

[21] L. Piancastelli, M. Gardella, S. Cassani. 2017. Cooling System Optimization For Light Diesel Helicopters. Journal of Engineering and Applied Sciences. ISSN 1819-6608, 12(9): 2803-2808, EBSCO Publishing, 10 Estes Street, P.O. Box 682, Ipswich, MA 01938, USA.

[22] L. Piancastelli, S. Cassani. 2017. Study And Optimization Of A Contra-Rotating Propeller Hub For Convertiplanes. Part 1: Vto And Hovering. Journal of Engineering and Applied Sciences. ISSN 1819-6608, 12(11): 3451-3457, EBSCO Publishing, 10 Estes Street, P.O. Box 682, Ipswich, MA 01938, USA.

[23] L. Piancastelli, S. Cassani. 2017. On The Conversion Of Automotive Engines For General Aviation. Journal of Engineering and Applied Sciences. ISSN 1819-6608, 12(13): 4196-4203, EBSCO Publishing, 10 Estes Street, P.O. Box 682, Ipswich, MA 01938, USA.

[24] L. Piancastelli, S. Cassani. 2017. Convertiplane Cruise Performance With Contra-Rotating Propeller. Journal of Engineering and Applied Sciences. ISSN 1819-6608, 12(19): 5554-5559, EBSCO Publishing, 10 Estes Street, P.O. Box 682, Ipswich, MA 01938, USA.

[25] L. Piancastelli, S. Cassani. 2017. Tribological Problem Solving in Medium Heavy Duty Marine Diesel Engine Part 1: Journal Bearings. Journal of Engineering and Applied Sciences. ISSN 1819-6608,

12(22): 6533-6541, EBSCO Publishing, 10 Estes Street, P.O. Box 682, Ipswich, MA 01938, USA.

[26] A. Ceruti, T. Bombardi, T., and L. Piancastell. 2016. Visual Flight Rules Pilots Into Instrumental Meteorological Conditions: a Proposal for a Mobile Application to Increase In-flight Survivability. International Review of Aerospace Engineering (IREASE). 9(5).